Nuclear Engineering and Technology 49 (2017) 1100–1108

Contents lists available at ScienceDirect

Nuclear Engineering and Technology

journal homepage: www.elsevier.com/locate/net

Technical Note

Modification of the fast fourier transform-based method by signal mirroring for accuracy quantification of thermal-hydraulic system code

Tae Wook Ha [a], Jae Jun Jeong [a, *], Ki Yong Choi [b]

[a] School of Mechanical Engineering, Pusan National University, 2, Busandaehak-ro 63beon-gil, Geumjeong-gu, Busan, 46241, South Korea
[b] Korea Atomic Energy Research Institute (KAERI), 111, Daedeok-daero 989 beon-gil, Yuseong-gu, Daejeon, 34057, South Korea

ARTICLE INFO

Article history:
Received 13 November 2016
Received in revised form
10 February 2017
Accepted 24 March 2017
Available online 15 May 2017

Keywords:
Cut-Off Frequency
Fast Fourier Transform-Based Method by Signal Mirroring
Frequency-Dependent Evaluation

ABSTRACT

A thermal–hydraulic system code is an essential tool for the design and safety analysis of a nuclear power plant, and its accuracy quantification is very important for the code assessment and applications. The fast Fourier transform-based method (FFTBM) by signal mirroring (FFTBM-SM) has been used to quantify the accuracy of a system code by using a comparison of the experimental data and the calculated results. The method is an improved version of the FFTBM, and it is known that the FFTBM-SM judges the code accuracy in a more consistent and unbiased way. However, in some applications, unrealistic results have been obtained. In this study, it was found that accuracy quantification by FFTBM-SM is dependent on the frequency spectrum of the fast Fourier transform of experimental and error signals. The primary objective of this study is to reduce the frequency dependency of FFTBM-SM evaluation. For this, it was proposed to reduce the cut off frequency, which was introduced to cut off spurious contributions, in FFTBM-SM. A method to determine an appropriate cut off frequency was also proposed. The FFTBM-SM with the modified cut off frequency showed a significant improvement of the accuracy quantification.

1. Introduction

The assessment of a thermal–hydraulic system code involves a comparison of calculated results against experimental data from separate effect tests and integral effect tests. The fast Fourier transform-based method (FFTBM) is a tool to quantitatively conduct such comparisons [1]. The method can show a discrepancy between experimental data and calculated results in the frequency domain and is known to be effective at assessing the code accuracy.

Many improvements to the FFTBM have been made since its first development. For a more complete picture of thermal–hydraulic code accuracy, Prošek and Mavko [2] devised an FFTBM with new accuracy measures. In another study by Prošek and Mavko [3], the capability to calculate a time-dependent accuracy was described. These improvements were used to quantify the accuracy of the code calculations for a large-break loss-of-coolant accident in the RD-14M facility [4]. Prošek and Leskovar [5] showed how FFTBM, with the capability to calculate time dependent code accuracy, could be successfully adapted for use within a severe accident field. Prošek et al. [6] proposed an FFTBM by signal mirroring (FFTBM-SM). By eliminating the so-called edge effect related to the discontinuity in FFTBM, the method significantly improved the capability to calculate code accuracy. It is known that the FFTBM-SM judges the accuracy in a more consistent and unbiased way.

However, in some applications, quantitative results obtained by raw experimental signal are considerably different from those obtained by noise-reduced experimental signal, although the obtained quantitative results are expected to be similar because the two signals are almost the same to code users. This reveals that, in the FFTBM-SM application, the accuracy quantification is dependent on whether noise exists in the experimental signal. In this study, it is identified that accuracy quantification by FFTBM-SM, as well as by FFTBM, is dependent on the frequency spectrum that is obtained by FFT of the experimental and error signals, meaning the difference between the experimental data and the calculated results. If the signals include a lot of noise as well as sharp changes or discontinuities, the frequency spectrum determined by FFT of the signals involves a lot of high-frequency components. Then, the high-frequency components have significant influence on the accuracy quantification, leading to frequency-dependent evaluation.

* Corresponding author.
E-mail address: jjjeong@pusan.ac.kr (J.J. Jeong).

http://dx.doi.org/10.1016/j.net.2017.03.010

So far, by using signal mirroring to eliminate the discontinuity causing the high-frequency components, FFTBM-SM has solved this problem in terms of the discontinuity only. Therefore, a further improvement is needed.

The objective of this work is to reduce the frequency dependent evaluation feature of FFTBM-SM. It is shown that, by reducing the cut off frequency, which has generally been set at 0.5 Hz, the problem could be mitigated by eliminating spurious high-frequency components. In this study, a method to determine an appropriate cut off frequency is proposed and its effect is demonstrated using the advanced thermal-hydraulic test loop for accident simulation (ATLAS) tests [7–9] calculations.

2. FFTBM for accuracy quantification

2.1. FFTBM

In FFTBM, the FFTs of the experimental and the error signals are performed first. The accuracy of a single variable is assessed by using the average amplitude (AA), which is defined by

$$AA = \frac{AA_{error}}{AA_{exp}} = \frac{\sum_{n=0}^{2^m} \left|\tilde{\Delta F}(f_n)\right|}{\sum_{n=0}^{2^m} \left|\tilde{F}_{exp}(f_n)\right|} \quad (1)$$

where $\left|\tilde{\Delta F}(f_n)\right|$ is the amplitude obtained by the FFT of the error signal at frequency f_n (where n=0,1, …,2^m and m is the exponent defining the number of points $N=2^{m+1}$ where m=8, 9, 10, 11) and $\left|\tilde{F}_{exp}(f_n)\right|$ is the amplitude obtained by the FFT of the experimental signal at f_n [10]. AA in Eq. (1) means the ratio of the sum of the amplitudes of the error signal to the sum of the amplitudes of the experimental signal. If the experimental and calculated signals are equal (i.e., the error signal is zero), AA becomes zero, which means perfect agreement. Inversely, if the calculated signal is zero, AA becomes 1.0, which means 100% error.

A cut-off frequency (COF) has been introduced to cut off spurious contributions, generally negligible. When calculating AA in Eq. (1), amplitudes above COF are neglected. Generally, the COF has been set at 0.5 Hz [11] because, in most cases, AA fully converges to AA at the highest (maximum) frequency within 0.5 Hz. The maximum frequency is defined by:

$$2f_{max} = \frac{2^{m+1}}{T_d} = \frac{N}{T_d} \quad (2)$$

where N is the number of sampled points, equally spaced, which is a power with base 2 (N range from 2^9 and 2^{12}) and T_d is the selected time window. In this study, N is determined such that f_{max} is > 0.5 Hz for each FFTBM application.

2.2. FFTBM-SM

FFTBM-SM was proposed by Prošek et al. [6] to improve a deficiency of FFTBM. For example, the integrated break flow signal, which is an experimental signal of the main steam line break experiment at the ATLAS facility [9], is presented in Fig. 1A. According to the periodic nature of the discrete Fourier transform (DFT) [12], the signal is considered as the periodically extended signal infinitely in DFT, as shown in Fig. 1B. Then, when the first data point differs from the last one in the original signal, a discontinuity is observed. The discontinuity yields several harmonic components in the frequency domain. Thus, the sum of amplitudes increases and AA is affected by this.

FFTBM-SM uses the symmetrized signal as presented in Fig. 2A rather than the original signal shown in Fig. 1A. FFTBM using a symmetrized signal that is a combination of the original signal and its mirrored signal; this signal does not result in the discontinuity when the symmetrized signal is periodically extended, as can be seen in Fig. 2B. Because of this, FFTBM-SM can judge the accuracy of a single variable in a more consistent and unbiased way than FFTBM [6].

3. Modification of FFTBM-SM

3.1. Frequency-dependent evaluation feature of FFTBM-SM

In this study, the limitation of FFTBM-SM is found; it can be described by the following example. Using a lag compensator, the signal in Fig. 2 can be processed into a noise-reduced signal. Fig. 3 shows the symmetrized signal and the noise-reduced symmetrized signal. Assume that the two signals are quantitatively assessed. Then, we would probably judge that the accuracy quantification obtained by FFTBM-SM should be almost the same as the area below the curve is almost the same. However, a different assessment based on the sum of the amplitudes, which is an index for accuracy quantification in FFTBM-SM, was obtained as shown in Table 1.

The Parseval relationship [13], which is one of the properties of DFT, states that the energy or power in the time-domain representation is equal to the energy or power in the frequency-domain representation:

$$\frac{1}{N}\sum_{n=0}^{2^{m+1}} |x[n]|^2 = \sum_{n=0}^{2^{m+1}} \left|\tilde{F}(f_n)\right|^2, \quad (3)$$

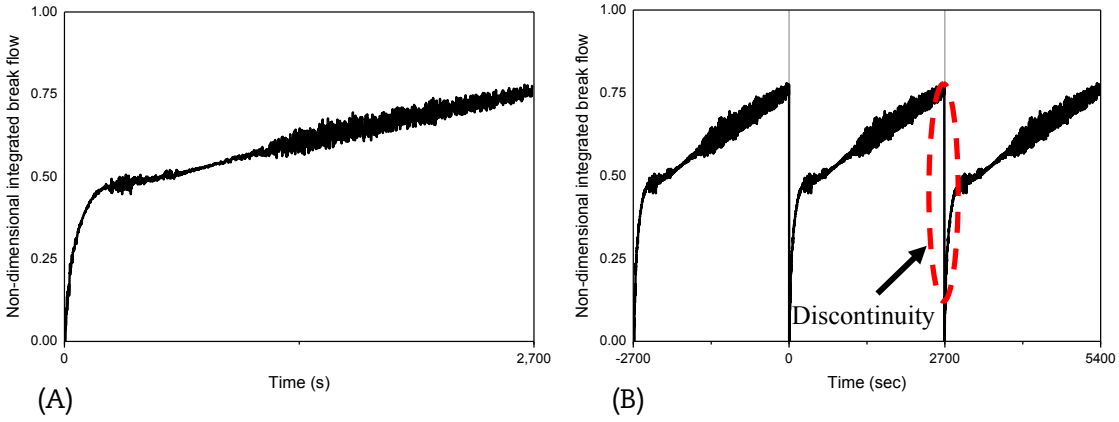

Fig. 1. Original signal and its periodically extended signal. (A) Symmetrized signal; (B) periodically extended signal.

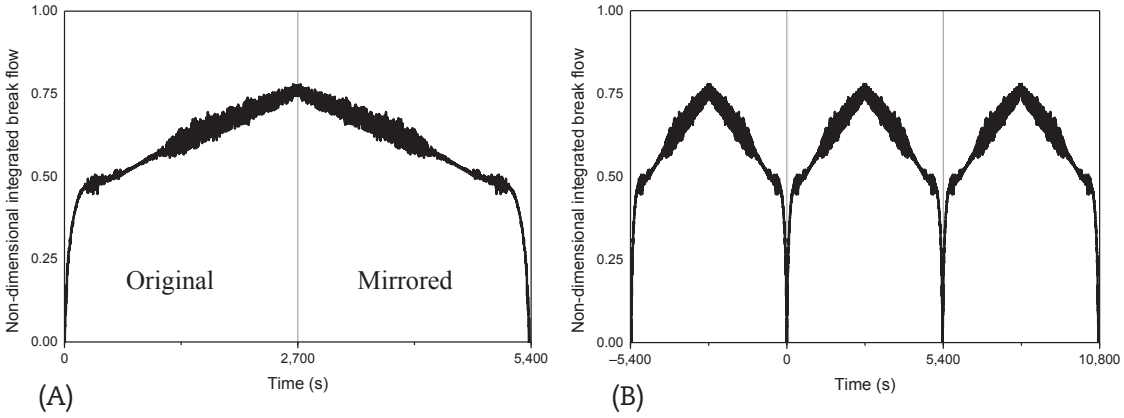

Fig. 2. Symmetrized signal and its periodically extended signal. (A) Symmetrized signal; (B) periodically extended signal.

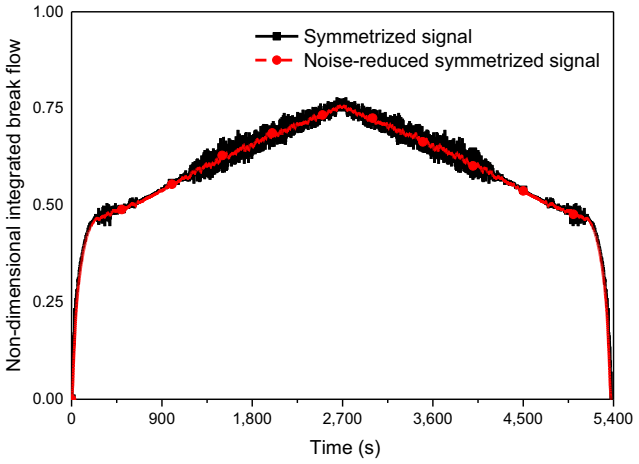

Fig. 3. Symmetrized and its noise-reduced signals.

where $x[n]$ is the n^{th} sampled value in the time domain of a signal and $F(f_n)$ is the n-th amplitude obtained by DFT of the signal. From Eq. (3), the sum of the square values in the time domain is preserved in the frequency domain. Thus, the sum of the square amplitudes, which is the right-hand side in Eq. (3), is almost the same for the symmetrized signal and its noise reduced signal, as shown in Table 1. However, the sum of the amplitudes in frequency domain is not preserved in the time domain and, thus, FFTBM and FFTBM-SM often show distorted accuracy quantification, such as in the above example. The cause of this problem is that accuracy quantification is dependent on the frequency spectrum of a signal. Fig. 4 shows the sums of the amplitudes of both signals versus the COF. As the COF increases, the sum of the amplitudes of the symmetrized signal continuously increases due to the influence of the high-frequency components caused by the large amount of noise. Meanwhile, the sum of the amplitudes of the noise-reduced symmetrized signal does not increase because the noise-reduced signal has few high-frequency components. When the COF is set at 0.5 Hz, the sum of the amplitudes is considerably different depending on how many high-frequency components affect it, although the accuracy quantification of both signals is expected to be similar.

Table 1
Sums of amplitudes and square amplitudes.

Type of signal	Sum of amplitudes	Sum of square amplitudes
Symmetrized signal	1.95×10^3	9.31×10^5
Noise-reduced symmetrized signal	1.45×10^3	9.21×10^5

The high-frequency components are produced by FFT of a signal that includes noise, sharp changes, and discontinuities. FFTBM-SM solved the problem related to the discontinuity only. If a signal includes noise or sharp changes, high-frequency components will affect the sum of the amplitudes excessively, leading to an inconsistent judgment.

3.2. FFTBM-SM with a reduced COF

Fig. 4 shows that, as the COF decreases, the difference between the sums of the amplitudes of both signals is gradually reduced. This implies that, by removing the excessive contribution of the high-frequency components, FFTBM-SM can provide consistent judgment regardless of noise or sharp changes. Therefore, we propose to reduce the COF of FFTBM-SM appropriately.

In the following subsections, tests and calculations are presented for FFTBM-SM applications. Then, it is discussed how much we have to reduce the COF.

3.2.1. Description of sample calculations

For FFTBM-SM applications, two cold-leg break loss-of-coolant accidents and a steam line break test conducted at the ATLAS facility [7–9] were selected. The ATLAS is a half-height and 1/288 volume scaled test facility with respect to the APR1400 (Advanced

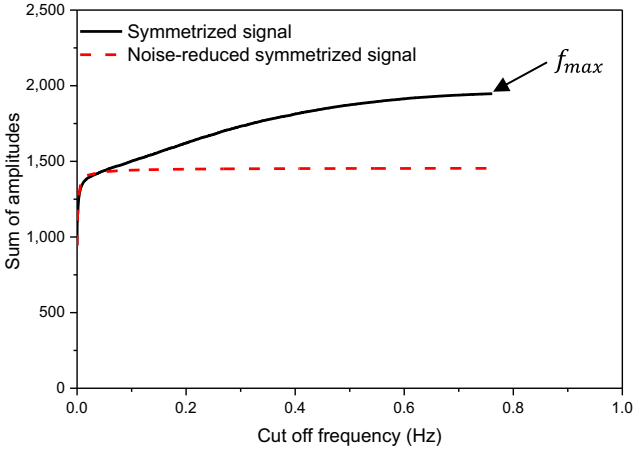

Fig. 4. Sum of amplitudes versus cut-off frequency. f_{max}, maximum frequency.

Table 2
Variables selected for fast Fourier transform-based method by signal mirroring applications.

ID	Cold leg break (Bottom) ATLAS SB-CL-09	Cold leg break (Top) LTC-CL-04R	Steam line break (SLB-GB-02T)
P1	Pressurizer pressure		
P2	SG-1 pressure		
P3	SG-2 pressure		
P4	Core inlet temperature		
P5	Core outlet temperature		
P6	Downcomer collapsed water level	Core collapsed water level	Pressurizer water level
P7	Mass flow rate of cold leg-1A	Mass flow rate of cold leg-1A	Mass flow rate of hot leg-1
P8	Mass flow rate of cold leg-2A	Mass flow rate of cold leg-2A	Mass flow rate of hot leg-2
P9	Break flow	Break flow	Integrated break flow
P10	Integrated break flow	Peak cladding temperature	SG-1 Water level
P11	Mass flow rate of Safety injection pump (SIP)-1	Mass flow rate of Safety injection pump (SIP)-1	SG-2 Water level

ATLAS, advanced thermal-hydraulic test loop for accident simulation; SG, steam generator.

Table 3
Information used for fast Fourier transform-based method by signal mirroring applications.

Input	Cold leg break (Bottom) SB-CL-09	Cold leg break (Top) LTC-CL-04R	Steam line break SLB-GB-02T
N	2^{13}	2^{15}	2^{13}
T_d (sec)	2000	8693	2689
f_{max} (Hz)	1.024	0.942	0.762

f_{max}, maximum frequency; T_d, selected time window.

Power Reactor 1400 MWe), which is a pressurized water reactor equipped with two hot legs, four cold legs, and two steam generators (SGs). The three tests were calculated using the MARS (Multidimensional Analysis of Reactor Safety) code [14]. Table 2 shows 11 key variables for each test. *N*, T_d, and f_{max}, used for FFTBM-SM applications, are listed in Table 3.

3.2.2. Suggestion of an appropriate COF

Figs. 5–7 show AA values calculated with FFTBM-SM (AA_{SM}) versus the COF for each test. Depending on the COF, the behavior of AA_{SM} can be systematically explained by classifying the 11 variables into two groups depending on whether the signal of a variable includes noise and sharp changes or not. The first group is comprised of variables that do not include noise or sharp changes in experimental and error signals (these are called smooth variables). The remaining variables belong to the second group. Commonly, an AA_{SM} at COF of 0Hz (AA_{SM}^{0Hz}) is equivalent to the percentage error. As COF increases, the percentage error gradually converges to AA_{SM} at f_{max} ($AA_{SM}^{f_{max}}$), which was defined in Eq. (1). However, the process leading to convergence is slightly different for each group. In the case of the first group, the AA_{SM} values shown in Figs. 5–7A rapidly converge to $AA_{SM}^{f_{max}}$. In the case of the second group shown in Figs. 5–7B, the behavior of AA_{SM} is rather complicated and the AA_{SM} values slowly converge to $AA_{SM}^{f_{max}}$ due to the contribution of high-frequency components. Meanwhile, it can be commonly observed in the both groups. There are two distinct regions: one is the transition region, where the value of AA_{SM} rapidly changes with increasing COF in the low COF region. The other is the convergence region, in which the AA_{SM} values slowly converge to $AA_{SM}^{f_{max}}$. In the transition region, the value of AA_{SM} cannot be seen as an accuracy quantification with FFTBM-SM because the accuracy quantification defined in FFTBM-SM is the value of $AA_{SM}^{f_{max}}$. Thus, we propose to determine a COF at the boundary between the transition and the convergence regions. Once the COF is determined for each variable, we recommend the use of maximum COF determined among the variables. Because the resulting AA_{SM} can represent the $AA_{SM}^{f_{max}}$ for most of the variables, the effect of the high-frequency components causing the problem in FFTBM-SM can at the same time be properly reduced.

To determine the boundary, the derivative versus the COF for each test is presented in Fig. 8. Referring Figs. 5–7, as well as Fig. 8, a criterion is empirically suggested, as follows:

$$0 < \frac{dAA_{SM,i}}{dCOF} < 3 \quad \text{for } i = 1, 2, 3, \ldots N \tag{4}$$

where i is the i-th analyzed variable for each test. Because the values of AA_{SM} in Figs. 5–7 fluctuate very much locally, the derivative in Eq. (4) is sensitive to the sampled dCOF. For a more consistent determination of the appropriate COF (f_{app}), the dCOF was equally sampled at 0.001 Hz for each test. As shown in Fig. 8, for all tests, the values rapidly decrease as the COF increases from 0 Hz, that is, the values of AA_{SM} rapidly converge to $AA_{SM}^{f_{max}}$.

Fig. 9 shows the flow chart used to determine f_{app}. At first, $f_{app,i}$ is determined as the maximum COF that satisfies the criterion in Eq. (4) for each variable. Then, f_{app} is determined as the maximum COF

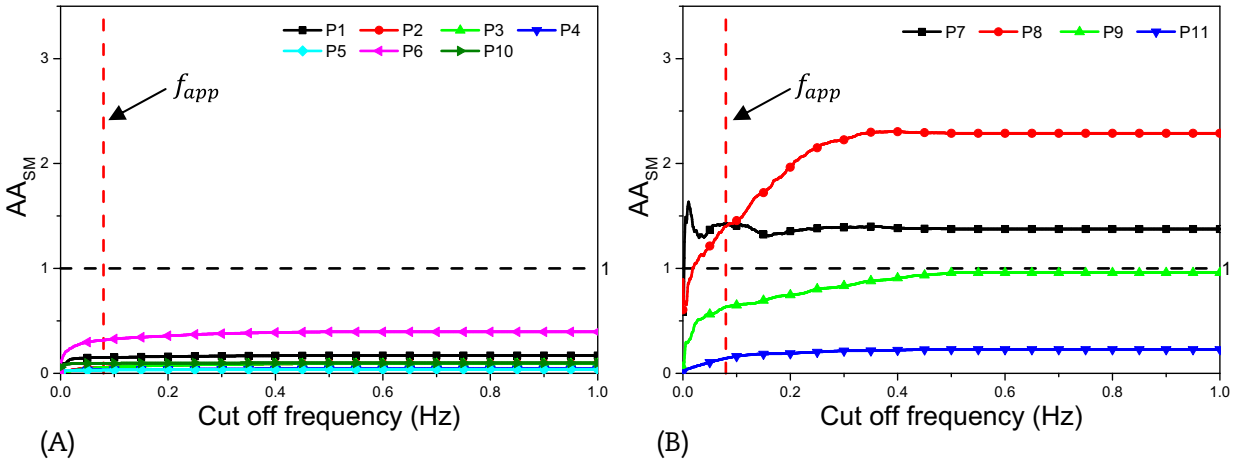

Fig. 5. AA_{SM} versus COF for cold leg break (bottom). (A) Smooth variables; (B) variables including noise or sharp changes. AA_{SM}, Average Amplitude values calculated with FFTBM-SM; f_{app}, appropriate cut-off frequency; FFTBM-SM, fast Fourier transform-based method by signal mirroring.

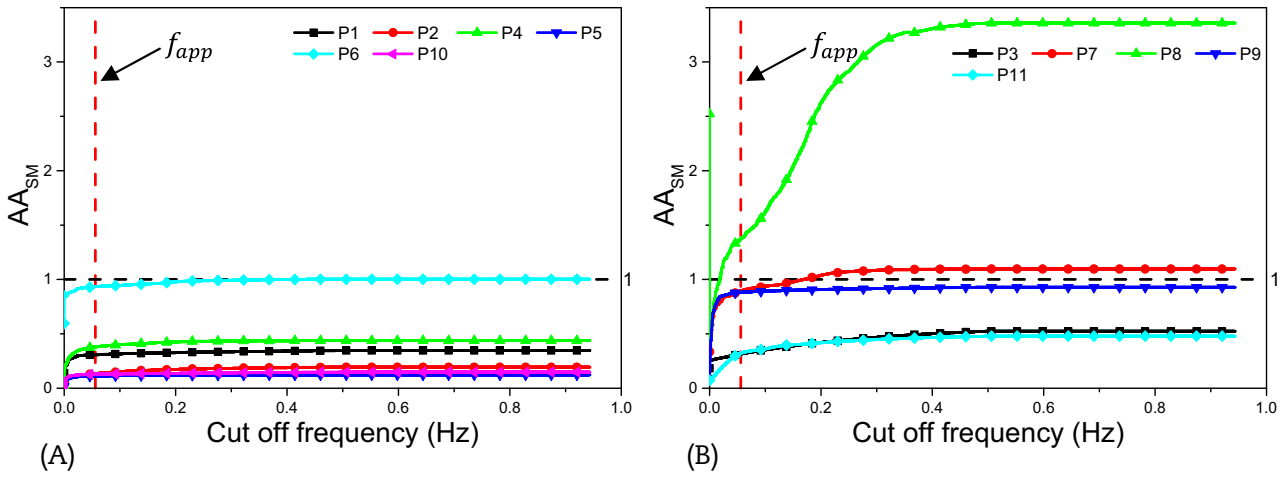

Fig. 6. AA_{SM} versus COF for cold leg break (top). (A) Smooth variables; (B) variables including noise or sharp changes. AA_{SM}, Average Amplitude values calculated with FFTBM-SM; f_{app}, appropriate cut-off frequency; FFTBM-SM, fast Fourier transform-based method by signal mirroring.

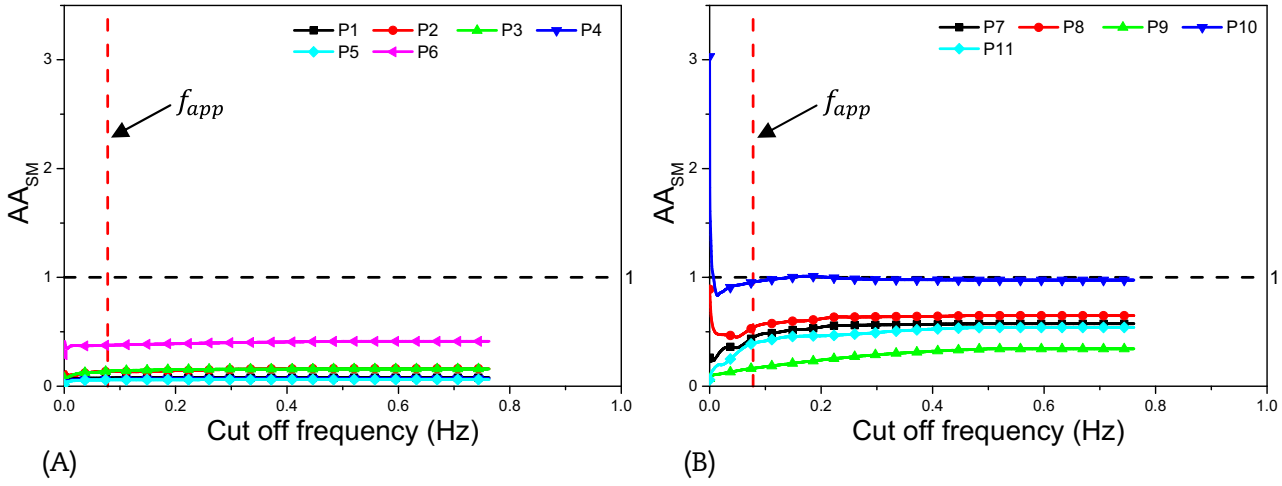

Fig. 7. AA_{SM} versus COF for ATLAS main steam line break. (A) Smooth variables; (B) variables including noise or sharp changes. AA_{SM}, Average Amplitude values calculated with FFTBM-SM; f_{app}, appropriate cut-off frequency; FFTBM-SM, fast Fourier transform-based method by signal mirroring.

among $f_{app,i}$ for the selected test. Exceptionally, the variables P7 and P8 in Fig. 5 and P7 and P8 in Fig. 6 were excluded in determining f_{app}. The accuracy quantification by FFTBM-SM is dependent on noise or sharp changes in experimental or error signals. These variables include a lot of noise and sharp changes and, thus, the values of AA_{SM} obtained by COF of 0.5 Hz are >1.0, which means 100% error. These variables may be not suitable or their accuracies could be considered to be 1.0 (100% error) for FFTBM-SM analysis. For each test, the determined f_{app} s are presented in Table 4.

4. Results using modified COFs

Comparing $AA_{SM}^{0.5Hz}$ and $AA_{SM}^{f_{app}}$, the advantages of FFTBM-SM using f_{app} can be described by three example cases: (i) Experimental or calculated signals include a lot of high frequency components caused by noise and the high frequency components can be removed by certain signal processing methods to reduce the noise. (ii) The signals originally include a lot of high frequency components and the high frequency components cannot be removed by signal processing methods. Generally, flow rate signals, including sudden changes caused by injection or release of water during a selected transient scenario, belong to this case. (iii) The signals do not originally include high frequency components as in the case of the smooth variables in the first group.

The case (i) example is the variable P3 for the cold leg break (top). As shown in Fig. 10, the experimental signal includes two sharp changes and was modified by eliminating the sharp changes. Comparing both experimental signals and the calculated signal, $AA_{SM}^{0.056}$ and $AA_{SM}^{0.5}$ are respectively presented in Table 5. We may expect similar accuracy quantification for the two comparisons. However, the value of $AA_{SM}^{0.5}$ in Table 5A is quite large compared to that in Table 5B because the accuracy quantification with a COF of 0.5 Hz is considerably dependent on high-frequency components. Meanwhile, the difference between the two $AA_{SM}^{0.056}$ s was considerably reduced because FFTBM-SM using f_{app} is less sensitive to a signal frequency for the accuracy quantification. Similarly, another example is the variable P9 for the main steam line break, shown in Fig. 11. As mentioned earlier, the experimental signal was processed into a noise-reduced signal through a lag compensator. Comparing the two experimental signals and the calculated signal, $AA_{SM}^{0.078}$ and $AA_{SM}^{0.5}$ are respectively presented in Table 6. The difference between the two values of $AA_{SM}^{0.078}$ was significantly reduced compared to the difference between the two $AA_{SM}^{0.5}$s values. From both examples, we confirm that FFTBM-SM using f_{app} can show more consistent

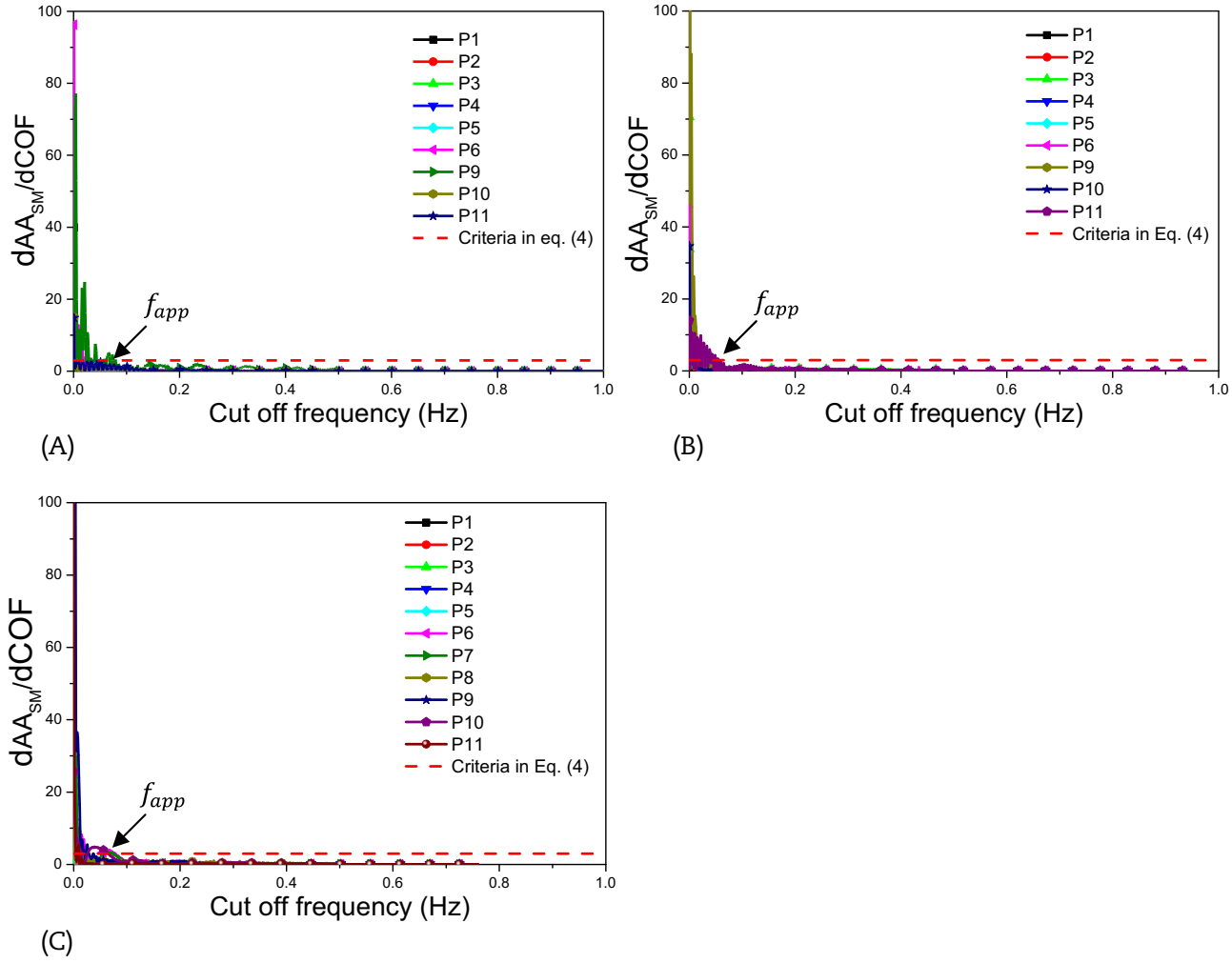

Fig. 8. Derivative in Eq. (4) versus cut-off frequency for each test. (A) ATLAS Cold leg break (bottom); (B) ATLAS cold leg break (top); (C) ATLAS main steam line break. dAA_{SM}, difference between AA_{SM}s at two sampled cut-off frequencies; dCOF, difference between two sampled cut-off frequencies; f_{app}, appropriate cut-off frequency.

judgment regardless of sharp changes or noise in the experimental signal.

The case (ii) example is the variable P11 for the cold leg break (bottom), shown in Fig. 12. The experimental signal was processed using the same method as that used for the variable P9 for the main steam line break. Comparing the two experimental signals and the calculated signal, the values of $AA_{SM}^{0.08}$ and $AA_{SM}^{0.5}$ are respectively shown in Table 7. Unlike the case (i) examples, the difference between the two $AA_{SM}^{0.5}$ values is quite small because the sharp change, causing the high frequency components, still exists in the noise-reduced experimental signal. In case (ii), because the experimental signal originally includes many high frequency components, the frequency dependency of FFTBM-SM cannot be improved by signal processing to reduce noise. Meanwhile, the difference between the two values of $AA_{SM}^{0.08}$ slightly increased compared to the difference between the two values of $AA_{SM}^{0.5}$. This may be because, through the lag compensator, the sharp change in the experimental signal was slightly distorted and the maximum error also changed from 0.3 to 0.24. This seems to have an influence on the difference between the two values of $AA_{SM}^{0.08}$.

In the case (ii) example, it should be noted that $AA_{SM}^{0.08}$ is considerably lower than $AA_{SM}^{0.5}$ in Table 7 A and the value of $AA_{SM}^{0.08}$ is an improved accuracy quantification. As shown in Fig. 12, there is good agreement when comparing the experimental and calculated signals. However, in the example, $AA_{SM}^{0.5}$ shows a fairly inconsistent result, that is, 0.229. In Fig. 11, we can observe a slight disagreement between the noise-reduced experimental and calculated signals, and $AA_{SM}^{0.5}$ in Table 6B shows a value of 0.179. When the two values of $AA_{SM}^{0.5}$ in Table 7 and 6 are compared, we recognize that Fig. 12 shows more disagreement than Fig. 11 but this is not true when comparing the two figures. The values of AA_{SM} by f_{app} are 0.169 and 0.143 in Tables 6 and 7, respectively. These results give a more consistent judgment than the results when using a COF of 0.5 Hz. It should be noted that $AA_{SM}^{0.5}$ in Table 6 is larger than $AA_{SM}^{0.5}$ in Table 7 because the raw experimental signal in Fig. 11 includes a lot of noise compared to the signal in Fig. 12.

In the previous FFTBMs applications [11,15], we were able to observe a considerable disagreement for the mass flow rate signals (e.g. hot leg and cold leg mass flow rates, break flow) rather than for the signals for smooth variables. The signals originally include a lot of high frequency components caused by rapidly changing mass flow rates. For these signals, the accuracy quantification by FFTBM-SM should be improved by using f_{app}, such as in the case (ii) example.

In case (iii), that is, in the case of using smooth variables, the accuracy quantification by $AA_{SM}^{0.5}$ was no problem. For the case (iii) example, the variable P10 for the cold leg break (bottom) is presented in Fig. 13. The experimental signal of variable P10 was also processed through a lag compensator, and the two signals and calculated signal were compared by FFTBM-SM. Because the experimental signal does not originally include high frequency

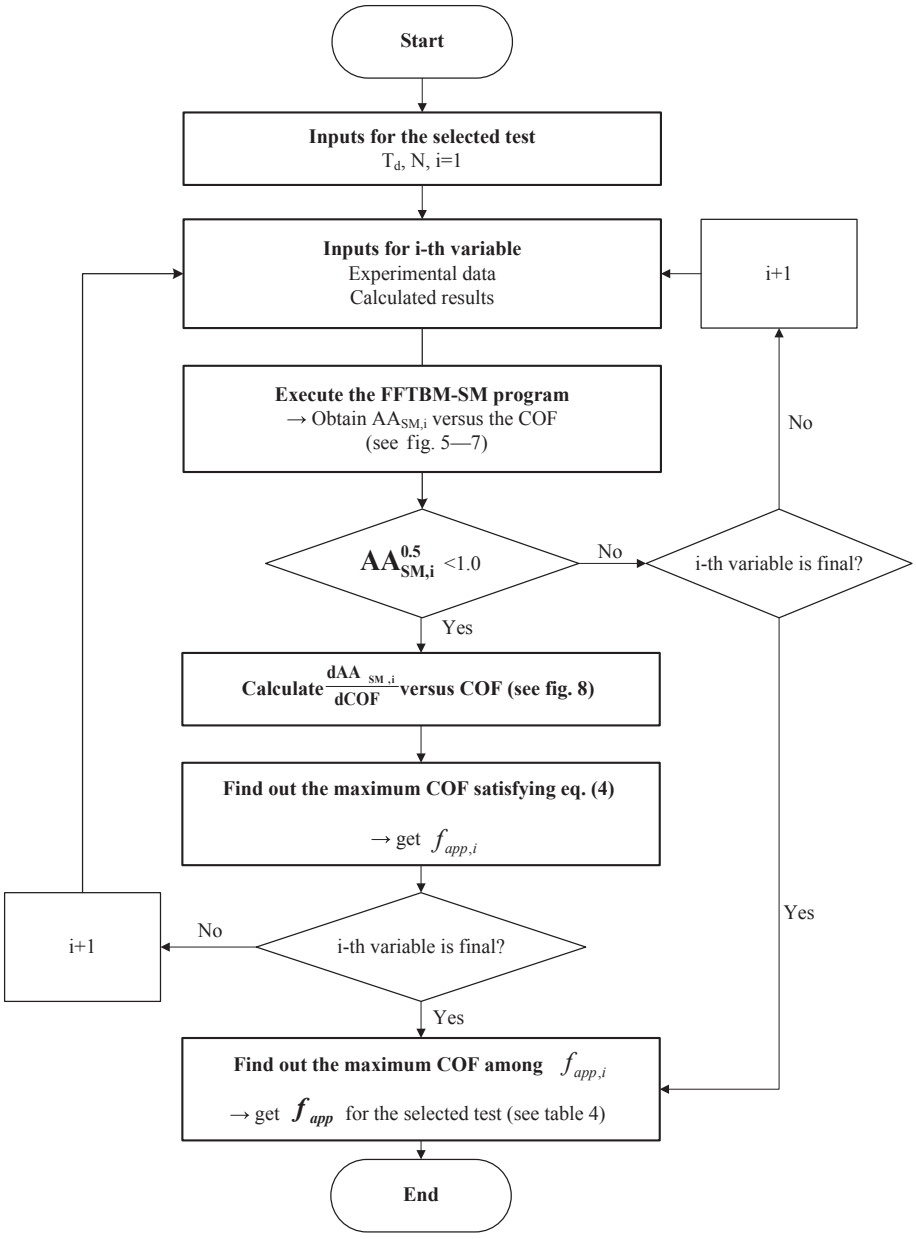

Fig. 9. Flow chart to determine f_{app}. $AA_{SM,i}$, Average Amplitude calculated with FFTBM-SM for *i*-th analyzed variable; COF, cut-off frequency; $dAA_{SM,I}$, difference between AA_{SM}s at two sampled cut-off frequencies for *i*-th analyzed variable; dCOF, difference between two sampled cut-off frequencies; $f_{app,i}$, appropriate cut-off frequency for *i*-th analyzed variable; FFTBM-SM, fast Fourier transform-based method by signal mirroring; i, number of analyzed variable; N, the number of sampled points; T_d, selected time window.

components, the values of $AA^{0.08}_{SM}$ and $AA^{0.5}_{SM}$ in Table 8 are almost the same. Therefore, both $AA^{0.5}_{SM}$ and $AA^{f_{app}}_{SM}$ provide a consistent judgment. It should be noted that the comparison in Table 6 also belongs to case (iii). Like this, FFTBM-SM using f_{app} for smooth variables will show accuracy quantification similar to that obtained when using a COF of 0.5 Hz. This is also an advantage of the use of f_{app}. If f_{app} approaches zero, the accuracy quantification will be significantly different from the results obtained by a COF of 0.5 Hz.

FFTBM-SM using f_{app} shows an improved accuracy quantification compared to the results obtained by FFTBM-SM with a COF of 0.5 Hz in cases (i) and (ii). In case (ii), the problem of FFTBM-SM cannot be solved by using the lag compensator to reduce noise; however, such problems can be solved by FFTBM-SM using f_{app}. f_{app} itself plays a role in eliminating high frequency components causing the problem. In case (iii), for the smooth variables, almost the same results are obtained. That is another advantage obtained by using f_{app}. From the results of these FFTBM-SM applications, it

Table 4
f_{app} for each test.

	Cold leg break (Bottom) ATLAS SB-CL-09	Cold leg break (Top) LTC-CL-04R	Steam line break (SLB-GB-02T)
f_{app}	0.08 Hz	0.056 Hz	0.078 Hz

ATLAS, advanced thermal-hydraulic test loop for accident simulation; f_{app}, appropriate cut-off frequency.

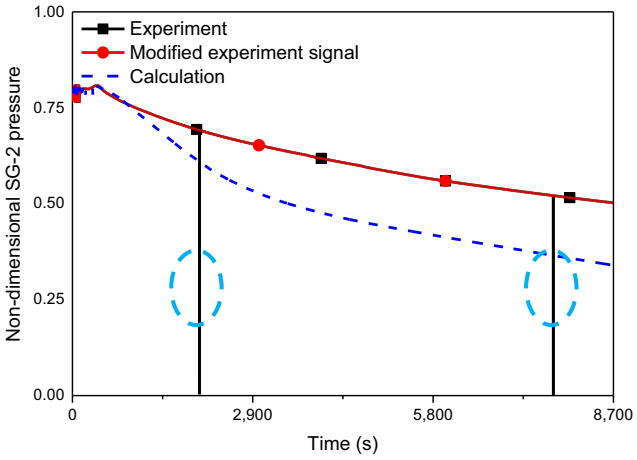

Fig. 10. Signals of P3 for cold leg break (top). SG, steam generator.

Table 5
AA_{SM} of P3 obtained using cut-off frequencies of 0.056 and 0.5 Hz for cold leg break (top).

Comparison	$AA_{SM}^{0.056}$	$AA_{SM}^{0.5}$
Original data and calculation	0.324	0.523
Noise-reduced data and calculation	0.284	0.343

AA_{SM}, Average Amplitude calculated with FFTBM-SM.

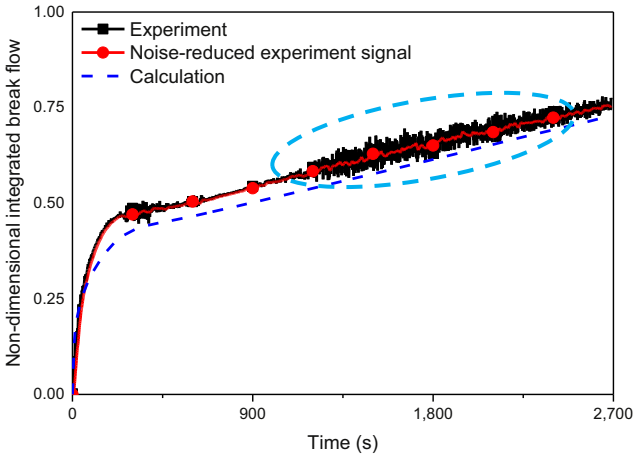

Fig. 11. Signals of P9 for steam line break.

can be said that FFTBM-SM with f_{app} shows improved accuracy quantification and, at the same time, represents the accuracy quantification obtained by original FFTBM-SM (using COF of 0.5 Hz).

Table 6
AA_{SM} of P9 obtained using cut-off frequencies of 0.078 and 0.5 Hz for the steam line break.

Comparison	$AA_{SM}^{0.078}$	$AA_{SM}^{0.5}$
Original data and calculation	0.164	0.343
Noise-reduced data and calculation	0.169	0.179

AA_{SM}, Average Amplitude calculated with FFTBM-SM.

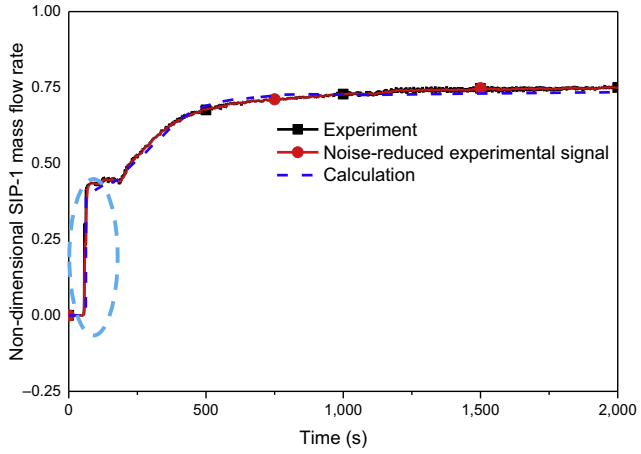

Fig. 12. Signals of P11 for cold leg break (bottom).

Table 7
AA_{SM} of P11 obtained using cut-off frequencies of 0.08 and 0.5 Hz for cold leg break (bottom).

Comparison	$AA_{SM}^{0.08}$	$AA_{SM}^{0.5}$
Original data and calculation	0.143	0.229
Noise-reduced data and calculation	0.105	0.209

AA_{SM}, Average Amplitude calculated with FFTBM-SM.

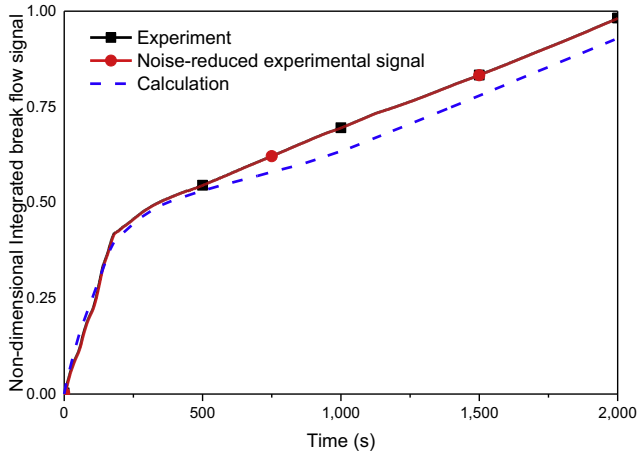

Fig. 13. Signals of P10 for cold leg break (bottom).

Table 8
AA_{SM} of P10 obtained using cut-off frequencies of 0.08 and 0.5 Hz the cold leg break (bottom). AA_{SM}.

Comparison	$AA_{SM}^{0.08}$	$AA_{SM}^{0.5}$
Original data and calculation	0.096	0.098
Noise-reduced data and calculation	0.098	0.099

AA_{SM}, Average Amplitude calculated with FFTBM-SM.

5. Concluding remarks

FFTBM-SM has been frequently used to quantify the accuracy of thermal–hydraulic system codes. In this study, we showed that accuracy quantification by FFTBM-SM with a COF of 0.5 Hz is considerably affected by high-frequency components caused by noise, sharp changes or discontinuities in experimental or error signals. To eliminate the effects of the high-frequency components, we propose to reduce the present COF in FFTBM-SM. Because

excessively reduced COF may result in other problems, we suggest a mathematical criterion to choose an appropriate COF, which represents a frequency at the boundary between the transition and the convergence regions in the AA_{SM}-versus-COF plane.

We finally show from the FFTBM-SM applications of the three ATLAS tests that the FFTBM-SM with the modified COF can produce more consistent judgment of the accuracy, regardless of noise and sharp changes, than the present FFTBM-SM.

Conflicts of interest

The authors have no conflicts of interest to declare.

Acknowledgments

This work was supported by the Nuclear Safety Research Program through the Korea Foundation of Nuclear Safety, granted financial resources by the Nuclear Safety and Security Commission (NSSC), Republic of Korea (No. 1305011).

References

[1] W. Ambrosini, R. Bovalini, F. D'Auria, Evaluation of accuracy of thermal-hydraulic code calculations, Energia Nucleare 7 (1990) 5–16.
[2] A. Prošek, B. Mavko, A tool for quantitative assessment of code calculations with an improved fast Fourier transform based method, Electrotech Rev. 70 (2003) 291–296.
[3] A. Prošek, B. Mavko, Quantitative assessment of time trends: influence of time window selection, in: Proceedings of the 5th International Conference on Nuclear Option in Countries with Small and Medium Electricity Grids, Dubrovnik, Croatia, 2004, pp. 1–9.
[4] A. Prošek, F. D'Auria, D.J. Richards, B. Mavko, Quantitative assessment of thermal–hydraulic codes used for heavy water reactor calculations, Nucl. Eng. Des. 236 (2006) 295–308.
[5] A. Prošek, M. Leskovar, Application of FFTBM to severe accidents, in: Proceedings of the International Conference on Nuclear Energy for New Europe, Bled, Slovenia, 2005, pp. 013.1–013.10.
[6] A. Prošek, M. Leskovar, B. Mavko, Quantitative assessment with improved fast Fourier transform based method by signal mirroring, Nucl. Eng. Des. 238 (2008) 2668–2677.
[7] K.Y. Choi, Y.S. Kim, K.H. Kang, S. Cho, H.S. Park, N.H. Choi, B.D. Kim, K.H. Min, J.K. Park, H.G. Chun, X.G. Yu, H.T. Kim, C.H. Song, S.K. Sim, S.S. Jeon, S.Y. Kim, D.G. Kang, T.S. Choi, Y.M. Kim, S.G. Lim, H.S. Kim, D.H. Kang, G.H. Lee, M.J. Jang, Comparison Report of Open Calculations for ATLAS Domestic Standard Problem (DSP-02), Korea Atomic Energy Research Institute, Daejeon, 2012.
[8] J.R. Kim, K.H. Kang, K.Y. Choi, Y.S. Park, B.U. Bae, Y.S. Kim, S. Cho, H.S. Park, N.H. Choi, K.H. Min, Y.C. Shin, Analysis Report on the Long Term Cooling Test for Cold Leg Top Slot Break, Korea Atomic Energy Research Institute, Daejeon, 2016.
[9] K.H. Kang, Y.S. Park, S. Cho, H.S. Park, K.Y. Choi, Y.S. Kim, N.H. Choi, K.H. Min, Y.C. Sin, C.H. Song, Test Report on the Guillotine Break of the Main Steam Line Accident Simulation with the ATLAS, Korea Atomic Energy Research Institute, Daejeon, 2012.
[10] A. Prošek, M. Leskovar, Use of FFTBM by signal mirroring for sensitivity study, Ann. Nucl. Energy 76 (2015) 253–262.
[11] A. Prošek, F. D'Auria, B. Mavko, Review of quantitative accuracy assessments with fast Fourier transform based method (FFTBM), Nucl. Eng. Des. 217 (2002) 179–206.
[12] S.W. Smith, The Scientist and Engineer's Guide to Digital Signal Processing, second ed., California, San Diego, 1999.
[13] S. Haykin, B. Van Veen, Signals and Systems, John Willey &Sons Inc., New York, 1999.
[14] J.J. Jeong, K.S. Ha, B.D. Chung, W.J. Lee, Development of a multi-dimensional thermal-hydraulic system code, MARS 1.3.1, Ann. Nucl. Energy 26.18 (1999) 1611–1642.
[15] A. Prošek, B. Mavko, Quantitative Code Assessment with Fast Fourier Transform Based Method Improved by Signal Mirroring, US NRC, 2009. NUREG/IA-0220.